

Impact Assessment of Railway Bridge Construction Schedule, based on 3D Geotechnical Finite Element Modeling

Edina Koch and Richard P. Ray

Széchenyi István University, Department of Structural and Geotechnical Engineering, Egyetem tér 1, 9026 Győr, Hungary
e-mail: koche@sze.hu, ray@sze.hu

Abstract: The increasing demand for high-speed railways has risen, to solve the "age-old" problem of bridge abutments, the step between the backfill and the bridge deck. Examples prove that inadequate technical solutions can generate damage that may require long-term speed restrictions or lead to short maintenance cycles, significantly increasing the total cost of ownership. The problems associated with the transition zones require complex analysis. The complex interaction of structural elements with different stiffnesses and different dynamic behavior varies over time due to the time-dependent behavior of the soil, and in addition, a bridge deck and its connecting elements can be constructed in several sequences. This study investigated a typical single-span railway bridge and its soil environment using PLAXIS 3D geotechnical finite element software. Different constitutive soil models were used to approximate the behavior of the bridge and the connecting elements. To model the soil behavior, the HS-small constitutive model was implemented. Loads of the structure are transferred onto the subsoil by 60 cm diameter piles modeled as embedded piles. Six different construction schedules were analyzed using time-domain analyses. The importance of high-speed railways was highlighted, and a 250 km/h train speed was applied, using dynamic analysis. The study focuses on the effect of different construction schedules on settlement, consolidation time, the behavior of the transition, and the substructure movements. The results of this study show that geotechnical approaches by themselves are not enough to solve the problem of the transition zone, highlighting the collaboration of geotechnical, structural and railway engineers.

Keywords: numerical modeling; railway bridge; time effect; transition zone

1 Introduction

Track or railway transitions are locations along the track characterized by an abrupt variation of their stiffness, such as rail tracks changing from stiff to soft structures or vice versa [1]. This abrupt change generates differential settlements and increased dynamic loading that expedites track degradation through the

progressive deterioration of track geometry and materials [2] [3]. The typical railway transition zone is the bridge approach that experiences sudden changes in track stiffness. Track structures on the embankment and bridge sides reveal different layer geometries and properties. Additionally, differential settlement of the foundation and unsupported ties have been found near bridge abutments [4]. These conditions significantly impact rider comfort and operational safety during operation. Railroaders have recognized that track geometry issues and differential movement at railway transitions present a significant challenge to track profile maintenance [5] [6]. The bump problem at the transition between the embankment and the bridge is an important concern for railways and highways. These bumps can lead to a rough riding surface, creating high-speed discomfort and high maintenance costs [7] [8]. Transitions should provide a gradual stiffness variation.

At the bridge abutments, the stiffness of the rail support suddenly changes, causing vertical accelerations in the passing vehicle and additional stresses on the rail. Even after a short period, the sum of these stresses leads to residual deformations in the substructure that degrade the track geometry [9].

According to the European Rail Research Institute [10], the factors that affect the behavior of the track in transition zones can be separated into four groups: (1) external to the track (axle loads, weather conditions, speed, and vibrations), (2) geotechnical issues (sub-grade and soil conditions), (3) structural conditions (bending stiffness, lateral movements and interaction between track and bridge) or (4) related to the track design and layout (stiffness, location of track dilation devices or presence of continuous welded rail).

Several different solutions for transition zones have been proposed and applied. These transitions smooth the stiffness variation between the "flexible" approach section and the "rigid" section over the structure. Transitions based on smoothing the stiffness variation on the "flexible" side include:

- Using oversized sleepers or changing their spacing
- Installing underlayments of hot-mix-asphalt, geotextiles, or soil-cement
- Adding rails, approach slabs, and others [5] [11]

Transitions based on lowering the stiffness on the "rigid" section include:

- Placing soft rail pads under sleeper pads
- Installing plastic sleepers
- Laying down ballast mats [12] [13]

According to Li and Davis [5], transition zones must address the specific stiffness issues of the track discontinuities to be effective. The behavior of the railway track and infrastructure under the combination of high speed and repetitive axle loadings evolves due to a complex soil-structure interaction problem that challenges geotechnical and structural R&D [14].

Many numerical studies have focused on the influence of the vertical stiffness variation on this problem [15-17]. However, few have addressed a more critical aspect: Differential settlement's impact and long-term development [18] [19]. Intrinsically, the complex interaction of structural elements with different stiffnesses and different dynamic behavior varies over time due to the time-dependent behavior of the soil. In addition, a bridge abutment and its approaching elements can be constructed in different sequences, and therefore the nature and direction of the interactions can vary. Time is perhaps the most critical factor in analyzing the interactions between abutments and bridges [20].

In current practice, bridge designers calculate the internal forces of the superstructure with structural finite element software. This technique usually separates the analyses of the superstructure, substructure, and specific aspects of the foundation. Generally, the superstructure software models the foundation and the soil environment by linear springs and replaces the backfill with an external load [21]. Such a model only crudely approximates the actual soil-structure interaction behavior. Moreover, superstructure designers usually ignore the effects of the construction sequence and time-dependent processes such as soil consolidation [22]. Modern three-dimensional geotechnical FEM packages can model the behavior of the soil more realistically by applying advanced constitutive models. They can consider drainage, initial stress conditions, unloading-reloading phases, and soil-structure interaction. For dynamic behavior, linear or non-linear time history analyses allow investigating wave propagation phenomena in the subsoil and their effects on the structure [23].

This paper presents a model and simulation results of a typical single-track railway bridge and its soil environment. This research investigated the effect of different construction schedules, focusing on the settlement, consolidation time, transition behavior, and substructure movements.

2 Methodology of Modeling

2.1 The Bridge and its' Soil-Environment

The basic model of the bridge and connecting longitudinal section of the open track appear in Figure 1. The typical soil environment generates a time-critical analysis for the construction schedule. A 10 m thick soft, medium plasticity clay layer overlays a 10 m thick saturated sand layer. The groundwater level lies at the surface of the upper layer. The dense sand embankment measures 5.3 m high with a 1:1.5 slope. The 15 m long backfill on the crest, lying behind the bridge abutments, was "built-up" from very dense sand. The effective thickness of the embedded ballast is 0.35 m.

The height of the bridge abutments aligns with the embankment, and parallel wing walls connect to them. Piles support the abutments, arranged in 2 rows of 3 piles, each with a center-center separation of 2.4 m. The piles measure 0.6 m-diameter and 11.2 m long. The software models the piles as embedded beam elements, typical for this problem [22]. Data from load tests and past performance determine the values of soil skin friction and toe resistance. The pile caps, bridge abutments, wing walls, and superstructure consist of concrete solid elements with a Young's modulus of $E=30$ GPa. The superstructure was constructed with steel support and railway bedding, with an opening of 15.6 m. To model the soil-structure interaction, interface elements were placed behind the abutment and the wingwalls, $R_{inter}=0.8$ were applied for the backfill. Based on several numerical modeling of pile load test, $R_{inter}=0.95$ was used for subsoil [22]. The model represented an integral bridge with rigid connections between the abutment and superstructure [24] [25]. The monolithic assembly of integral bridges eliminates the need for expansion joints and bearings [26].

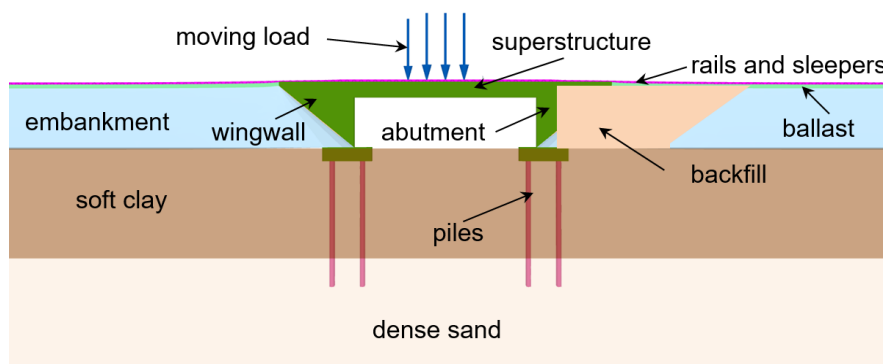


Figure 1

PLAXIS 3D model of the bridge and its soil environment

Beam elements represent rails with flexural and tensile rigidity based on their cross-section (60E1). The prestressed reinforced concrete sleepers (B70 type) are also modeled as beam elements with an adequate moment of inertia and cross-section. Table 1 lists input properties for the rails and sleepers. The sleepers were positioned in the model with a spacing of 60 cm intervals.

To analyze the effect of the model depth, 15 m, 20 m, and 25 m was investigated. For the selection of the applied model, the applied criteria for the incremental displacement was 1.0 mm. After the analysis, the overall model dimensions measure 96 m long, 75 m wide, and 20 m deep. The model contained 38466 elements and 62482 nodes with a mesh size of 2 m. Standard fixities and energy-absorbing boundaries reduced wave reflections in the domain.

The Hardening Soil model with small strain stiffness (HS-small) constitutive model was used to describe the soil behavior [27]. The input parameters for the medium-dense embankment and the dense backfill were determined based on [28]. Previous research provided properties of typical Hungarian soft clay [29] [30]. The ballast layer was modeled as elasto-plastic with Mohr-Coulomb yield parameters [31]; the reinforced concrete elements (pile cap, wing wall, bridge abutment) used a Linear Elastic model. The Poisson's ratio was $\nu = 0.2$ for all layers, as recommended by PLAXIS [23]. Similar to [31], static E moduli were applied for the different soil types. The geotechnical properties of soil layers appear in Table 2.

Table 1
Input parameters of rail and sleeper

Parameter	Sleeper B70	Rail 60E1
A (m ²)	0.0513	0.0077
\square (kN/m ³)	25	78
E (GPa)	36	200
I_3 (m ⁴)	0.0253	0.00003
I_2 (m ⁴)	0.00024	0.00000513

Table 2
Geotechnical properties of the layers

Parameter		Subsoil	Subsoil	Embankment	Backfill	Ballast
		Dense sand	Soft clay	Medium dense sand	Dense sand	Gravel
Model		HS-small	HS-small	HS-small	HS-small	MC
E	MPa					100.00
E_{50}^{ref}	MPa	51.00	6.00	36.00	48.00	
$E_{\text{oed}}^{\text{ref}}$	MPa	51.00	4.80	36.00	48.00	
$E_{\text{ur}}^{\text{ref}}$	MPa	153.00	24.00	108.00	144.00	
G_0^{ref}	MPa	117.80	40.00	100.00	114.40	
m	-	0.43	0.80	0.51	0.45	
$\square_{d,7}$	-	1.15E-4	2.5E-4	1.4E-4	1.2E-4	
c'_{ref}	kPa	1.00	30.00	1.00	1.00	10.00
\square'_{ref}	deg	39.00	25.00	35.50	38.00	40.00
ψ	deg	9.00		5.50	8.00	10.00
k	m/day	2.00	2E-4	1.00	2.00	10.00

2.2 The Construction and Load Phases

As mentioned, a bridge construction process could have various construction and loading phases due to different constraints or goals. The variants may have advantages and disadvantages regarding the construction time, the costs, and the displacements threatening the structure. Six different construction methods and schedule variants were chosen for analysis from many different options. In all variants, five construction stages were identical but occurred in different sequences for each variant:

1. Pile and abutment installation (also with deep mixing or vertical drains) duration of 10 days, always preceded Bridge Superstructure.
2. Bridge Superstructure 10 days.
3. Lower Embankment (0.0-2.6 m) 10 days, sometimes followed by consolidation time to 90% pore pressure reduction.
4. Upper Embankment (2.6-5.3 m) 10 days, sometimes immediately after Lower Embankment, always followed by consolidation time to 95% pore pressure reduction.
5. Ballast 10 days, Sleepers and Rails 10 days, Train Loading (always the final three stages in sequence).

Note that the consolidation stages were not precisely the same duration since the embankment sequence occurred at different times, either consecutively, or with other activities scheduled between the placement of the lower and upper portions. The consolidation stages' duration depended entirely on the average pore pressure reduction within the soil.

Each variant uses a slightly different sequence of construction in order to study their effect on the settlement and performance of the embankment and bridge. The six variants are listed below:

- Variant 1. Piles and Abutment, Bridge Superstructure Lower Embankment, 90% Consolidation, Upper Embankment, 95% Consolidation, Ballast, Sleepers and Rails, Train
- Variant 2. Piles and Abutment, Lower Embankment, 90% Consolidation, Upper Embankment, 95% Consolidation, Bridge Superstructure, Ballast, Sleepers and Rails, Train
- Variant 3. Lower Embankment, Rest Period of 60 days, Upper Embankment, Piles and Abutment, Bridge Superstructure, Backfill, 95% Consolidation, Ballast, Sleepers and Rails, Train

- Variant 4. Piles and Abutment, Lower Embankment, 90% Consolidation, Bridge Superstructure, Upper Embankment, 95% Consolidation, Ballast, Sleepers and Rails, Train
- Variant 5. Deep Soil Mixing, Piles and Abutment, Bridge Superstructure, Lower Embankment, Upper Embankment, 95% Consolidation, Ballast, Sleepers and Rails, Train
- Variant 6. Vertical Drains, Piles and Abutment, Bridge Superstructure, Lower Embankment, Upper Embankment, 95% Consolidation, Ballast, Sleepers and Rails, Train

Variants 5 and 6 require less consolidation time since the soft clays are stabilized by deep mixing or dissipate pore pressure more efficiently with vertical drains.

The consolidation stages use typical time-dependent behavior with coupled stress and pore pressure changes. The final train loading stage is a dynamic calculation.

The deep-mixing ground improvement was modeled as such: the improved material was regarded as a Linear Elastic model with $E=30$ MPa young modulus and much higher permeability, $k=8.6 \cdot 10^{-2}$ m/day. It can result from a cement or lime treatment carried out approximately in a 3.0×3.0 m, 60 cm diameter raster and 10 m length column [32]. The raster of the vertical drains is 2.0×2.0 m, and the length is bedded 1.0 m into the lower sand.

Figure 3 presents sketches showing the sequence of placement for the main components of the bridge and its soil environment.

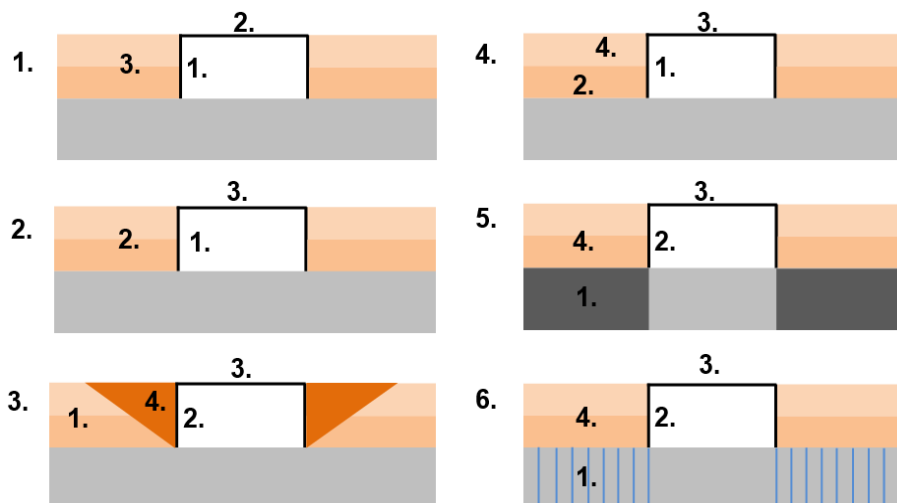


Figure 3

Schematic drawings of the investigated variants

The LM71 Eurocode load model represented the moving train with eight dynamic point loads of 125 kN vertical force [33]. PLAXIS 3D characterizes dynamic loads using a time-force signal. In the model, every dynamic point load has its multiplier, which turns the loads on and off, simulating the effects of the rolling vehicle. The dynamic time step must be changed to simulate different travel velocities while the distance between dynamic point loads is constant [31]. For analyzing the effect of the construction phases of a bridge construction, the vehicle's speed was set to 250 km/h. A train with 250 km/h speed passes 1.6 m in 0.023 sec; hence the time interval must be chosen 0.023 sec for the fixed dynamic point loads. The total elapsed time between the first and the last load was 1.3824 sec. An additional time of 0.6176 sec was considered to allow complete dissipation of the waves induced by the passing train.

3 Results Related to the Settlements

The final settlements of variant 1 are shown in Figures 4 and 5. These refer to the loading situation where the train reaches the middle of the bridge. The settlement behavior was similar for the other variants because the construction phases barely affected the final settlements, except for the ground improvement (variant 5). The essential settlement data are summarized in Table 3. The following conclusions can be made according to the Figures and the Table.

The open track has the most significant settlement, ~24 cm, which is obviously less in case of a ground improvement. Much less displacement can be seen behind the abutments, and directly behind the abutment, the settlement of the backfill is ~10-15% of the settlement of the open track. It is because the embankment fill is much smaller here because of the abutment and the sloped embankment, and the bridge abutment "supports" some of the embankment fill. Therefore, it can be stated that the settlement prognosis, based on the conventional calculation of settlement caused by the load due to the trapezoidal cross-section of the embankment, overestimates the settlements around the bridge abutment. The settlements behind the bridge abutment increase rapidly, at a distance of 3.5 m, generally about 60 mm, except variant 5, the applied ground improvement. Figure 5 shows that out of the ~24 cm of the open track's settlement, ~2.0 cm is the compression of the embankment, and ~1 cm is the subsidence of the sandy soil layer. The compression of the backfill is less than 1 cm. The bridge abutment and the superstructure exhibit negligible magnitudes of settlement (13-16 mm), which roughly corresponds to the settlement measurements of the abutments resting on a pile foundation.

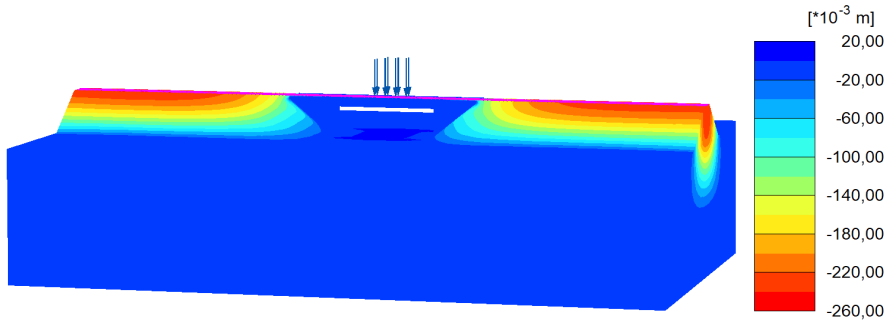


Figure 4
Vertical settlements for the construction schedule variant 1

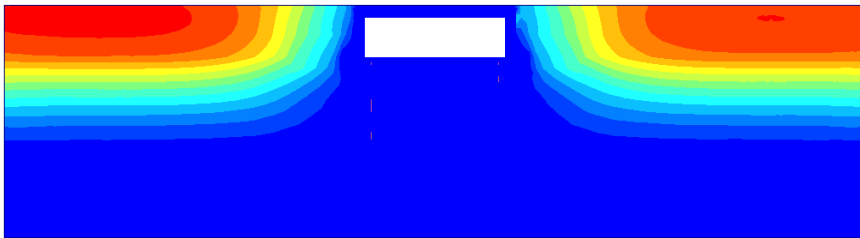


Figure 5
Longitudinal section of the bridge and its surroundings for the construction variant 1
(with the same scale of colors as Figure 3)

Table 3
The settlement of the track axis depending on the construction variants

Construction variants	Open track	Backfill from the bridge abutment		Bridge abutment
		to 4.0 m	to 0.5 m	
	mm			
1.	248.0	97.0	39.0	12.0
2.	249.0	96.0	30.0	13.3
3.	269.0	84.0	24.0	9.6
4.	246.0	95.0	28.0	9.6
5.	40.0	30.0	12.0	7.2
6.	257.0	102.0	38.0	11.4

4 Results of the Consolidation

Time may not play such an essential role in the case of a structure as the bridge abutment. Due to today's enforced construction time, there is no time to wait for the entire consolidation in most cases. Moreover, the project managers want an accurate prediction, which is difficult and impossible to produce. Poor predictions related to consolidation may cause problems with differential settlement in the bridge abutment and the backfill and generate negative skin friction within the piles.

The consolidation curves of the six different construction variants are shown in Figure 6. In order to be transparent, only those curves are shown, which were determined on the embankment surface, 20 m from the bridge abutment below the open track. The vertical displacement of the backfill zone, measured on the ground surface directly behind the abutment, is less than 2 cm; therefore, it is not shown in the figure. The full consolidation time of construction schedule variants 1, 2, and 4 is approximately 550 days; it is not significantly affected by the sequence of the superstructure's construction.

The immediate settlement is ~5 cm, followed by ~6 cm consolidation settlement due to the "consolidating time" of the lower embankment. These require about ~300 days. The second phase of the consolidation settlement due to the upper embankment is ~10 cm, and 200-250 days are necessary to reach a 95% degree of consolidation. The duration of the construction is approximately six months less in the case of variant 3 (the embankment of the open track is built before); however, the total consolidation settlement is 2 cm more. In the case of installing vertical drains into the subsoil (variant 6), the consolidation time is reduced by one-third, the embankment can be built in one phase, and the total consolidation settlement is ~25 cm. Following the expectations, the settlement and the consolidation time are drastically reduced in case of ground improvement (variant 5), and the embankment can be built in one phase.

Figure 6 also shows that the railway superstructure's construction induces further 5-8 mm incremental settlements after the complete consolidation. The settlement due to the train load, usually around 8 mm, is not presented in the figure but will be discussed separately later.

If the consolidation time exceeds 2-3 months, the settlement measurements are taken, and the construction phases can be set based on their results. According to Hungarian practice, the consolidation is considered to be "finished" if the settlement rate is below 1 cm/month. Figure 7 indicates the settlement rate of the same surface point as it was investigated regarding the settlement. Note that this rule's origin is unknown, but it can still be recognized in the geotechnical report of the bridge construction.

The figure clearly shows that the settlement rate suddenly increases when a new step of construction, e.g., the fill or sleepers' construction, starts. During the consolidation, the settlement rate decreases over time.

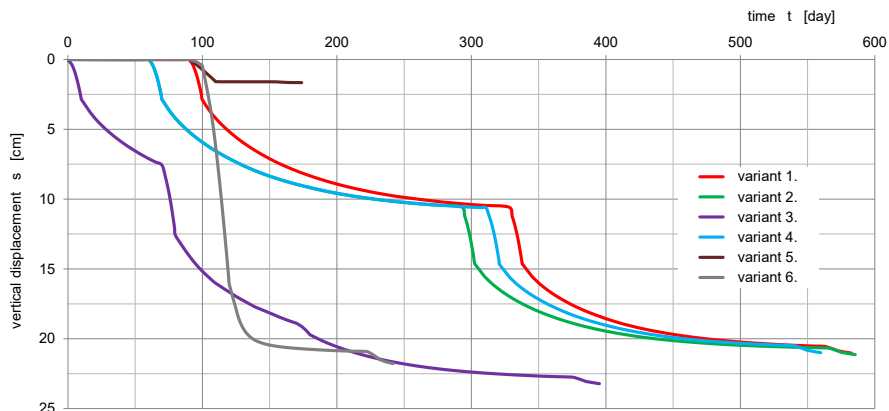


Figure 6

The consolidation of the open track concerning the construction variants

Variant 1 shows the slowest reduction of the settlement rate. After constructing the upper part of the embankment, the shape of the curves is similar in the case of variants 2 and 4, but variant 2 shows a slightly faster reduction. The sudden reduction can be observed in the case of variants 5 and 6 due to the prior ground improvement (deep mixing and vertical drains). For variant 3, the settlement rate reduction is relatively fast after the superstructure placement due to the early embankment construction.

The figure also shows that the settlements are still increasing even after the total (95% degree of consolidation) consolidation. Partly because it was not "full", partly as the railway superstructure also induces consolidation settlements, and partly due to the presence of the train load. The figure clearly confirms the false practice of the 1 cm/month rule; the expected incremental settlement is around 5 cm after reaching the given value.

This analysis aimed to show that the construction time can be optimized based on the total final settlement and the prediction of the settlement rate if the subsoil can be correctly parametrized. It could only happen in the case of a good soil analysis; however, such a prediction should also be based on the settlement measurements of the first construction phases.

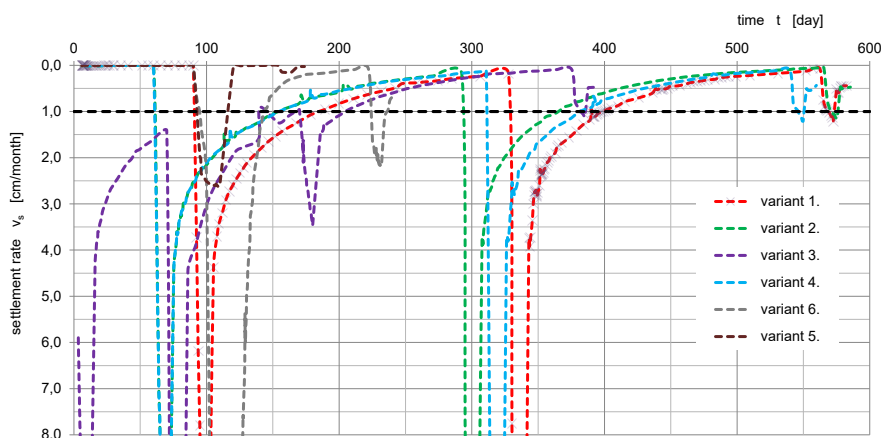


Figure 7

The settlement rate concerning the construction variants

5 Results Related to the Transition Zone

Analyzing the behavior of the transition zone was another goal of this study. Figure 8 shows the effect of the train load on the open track section (20 m from the abutment) and the backfill zone (0.5 m from the abutment). The selected points are located on the upper layer of the ballast. According to Figure 8, the train load produces twice the settlement on the open track (9-10 mm) when compared to settlement in the backfill (5 mm). The train induces permanent deformation (7-8 mm) remains after the train passes. In the case of variants 3, 5 and 6, the remaining settlement is slightly lower on the open track section than for variants 1, 2 and 4. In the backfill zone, the permanent settlement is around 2 mm.

The vertical settlements due to the train load are shown in the longitudinal profile in Figure 9. They have a lower magnitude near the bridge abutment and rapidly change directly behind it. It is because the bridge abutment barely settles under the train load. The effect of the train load is the smallest in the case of variant 3, likely due to the early construction of the embankment. In the case of ground improvement, the train load has the most considerable effect, likely due to the stiff subsoil. The curves are actually overlapping directly ~ 5 m behind the bridge abutment and show a settlement of ~ 7 mm. The deflection of the superstructure is around 3 mm; there is no significant difference in the case of the different variants.

Based on the results, it seems that the correct behavior of the last section in front of the bridge abutments cannot be solved only by applying geotechnical design.

In this case, according to the new Hungarian Railway Regulation, Volume 6 [34], a deck slab, such as a variation of the thickness of a high quality-balancing layer, as well as the reinforcement of the superstructure, e.g., additional rails or oversized sleepers, could help.

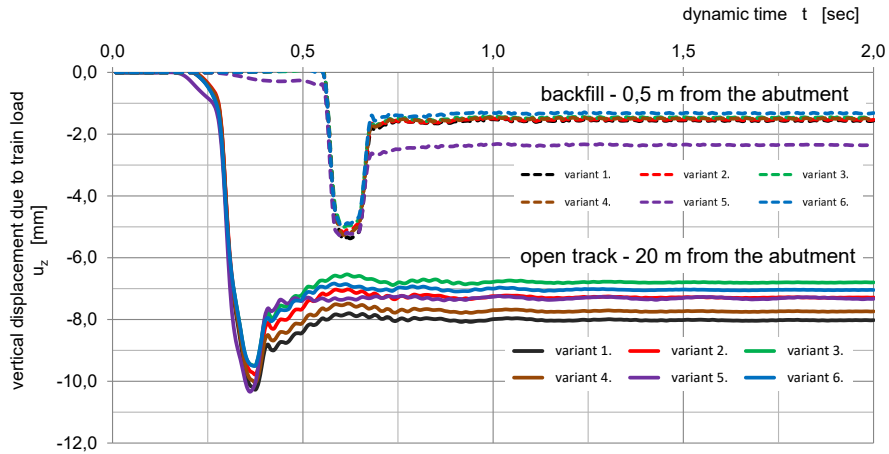


Figure 8

Vertical displacement due to the train load

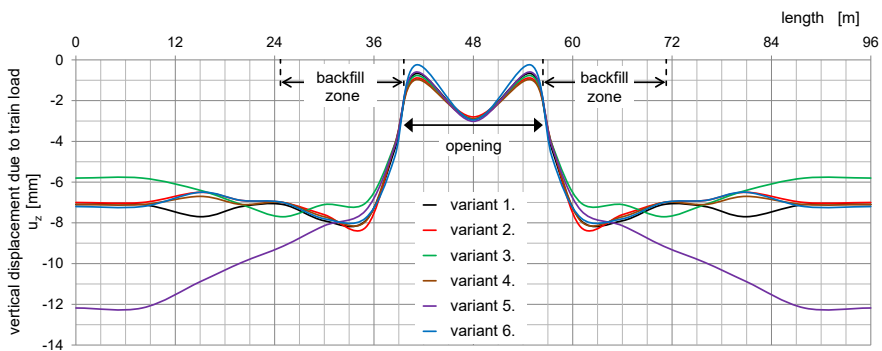


Figure 9

Vertical displacements due to the train load in each variant

6 Results Concerning the Substructure

Figure 10 illustrates the horizontal displacement of the bridge abutment before constructing the railway superstructure according to variant 1. In the figure, only the concrete pile cap, the bridge abutment, and the wing wall are visible for better

evaluation of displacements. The figure shows that the bottom of the wall moves towards the opening about 2 mm, while the top moves towards the embankment approximately 3.5 mm. Based on the middle part of the figure, it can be noted that the displacement of the bridge abutment is small, under 5 mm.

The horizontal displacements of the bridge abutment for the relevant construction phases are shown in Figure 11, related to variant 1. After constructing the superstructure, a horizontal displacement of approximately 2 mm can be seen, and the bridge abutment moves towards the embankment. Following the construction of the first step of the embankment, the top of the bridge abutment still moves towards the embankment, while the bottom moves towards the bridge. It can be observed that such a displacement is getting more significant in the following construction phases, and later, due to the trainload, the bridge abutment tilts towards the opening.

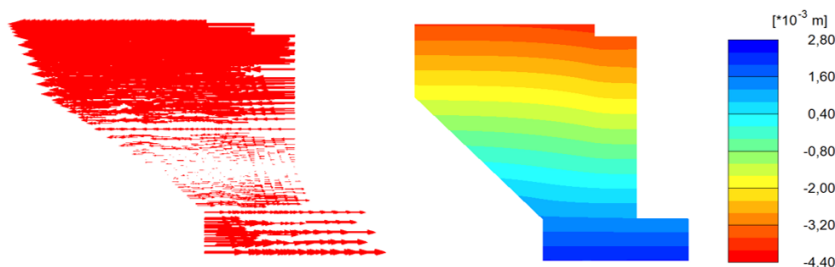


Figure 10
Horizontal displacement of the bridge abutment before constructing the beam

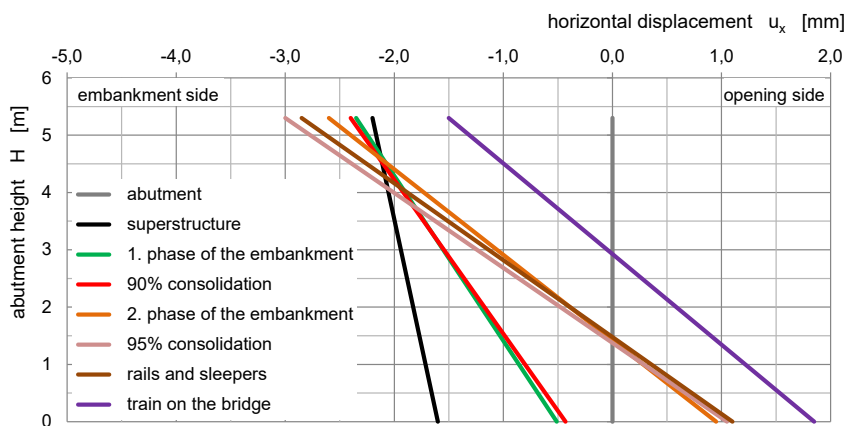


Figure 11
Horizontal movement of the bridge abutment concerning the construction phases (variant 1)

Figure 12 shows, according to the construction phases, the horizontal displacements of the bridge abutment relating to the state when the train load is above the abutment. Except for versions 2 and 4, the horizontal displacement of the bridge abutment seems to be quite similar; the extent of the displacement stays under 5 mm due to the early support. These displacements are about 0.1% of the height of the wall. The largest displacement, 20 mm, can be seen by variant 2; the bridge abutment wall moves totally towards the embankment, which induces a passive state in the backfill, and the wall gets strong support from it. The reason behind this is that the construction of the superstructure, together with the support of the abutments, begins after the consolidation; till then, the settlement of the embankment is dominant. The differential settlement induced by embankment consolidation near the base of the abutment causes its top to rotate into the embankment. Actually, the abutment fits into the bowl-shaped settlement depression. Construction phase variant 4 shows similar results, although the displacement is less because the support was created after constructing half of the embankment.

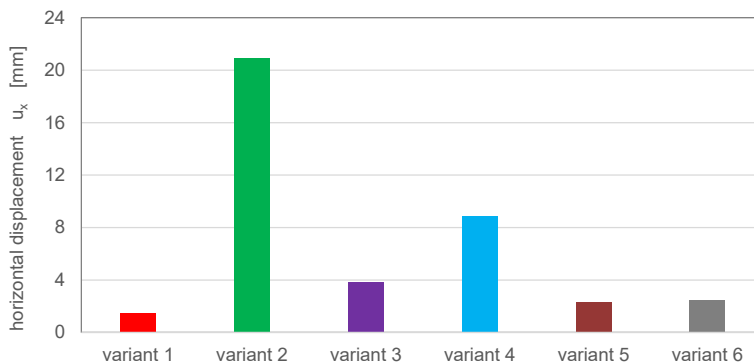


Figure 12

The displacement of the bridge abutment concerning the investigated variants

Conclusions

This study investigated a typical railway bridge and the related soil environment, focusing on the effect of different construction schedules. According to the analysis, several benefits and practical consequences could be concluded:

- Plaxis 3D software, applying the HS-small constitutive model and modeling the moving train, provides a realistic analysis of the current problem. It describes the global behavior of the railway bridge and its soil environment.
- Due to the spatial effects and a more realistic loading condition, the results of the settlements around the bridge abutment are more favorable, than the results derived from conventional analysis or 2D modeling.

- c) This type of modeling could allow for optimization of the construction process, the best sequence of construction phases, or the earliest date of construction of the railway superstructure.
- d) Due to the complex behavior of the bridge and its surroundings, we should not rely on simple design methods to provide a solution to the problem. The analysis presented here indicates the trends of soil and structural displacements, as well as the time required for adequate consolidation.
- e) The results showed that ground improvement could be a suitable technology to reduce construction time, but it is more costly. Using construction variant 1, 2, and 4 require the most time. Moreover, in the case of variant 2, horizontal displacement of the bridge abutment is might be greater than allowed; it may result in higher forces within the piles.
- f) Construction variant 3, reduces construction time and the cost is modest. The results related to the settlement, consolidation time, and horizontal movements of the bridge abutment are within reason.
- g) The results clearly show that geotechnical approaches, by themselves, are not sufficient to solve the problem of the transition zone. A holistic approach, combining geotechnical and railway superstructure tools, would produce a better transition between the bridge and the connecting embankment.

References

- [1] Varandas JN. *et al.* Three-dimensional non-linear modelling of railway tracks application to transition zones. INSERTZ, International Seminar on Rail Track Substructures and Transition Zones, Lisbon, Portugal, 2014
- [2] Indraratna B, Sajjad M. B, Ngo T, Correia A. G, Kelly R. Improved performance of ballasted tracks at transition zones: A review of experimental and modelling approaches, *Transportation Geotechnics*, Volume 21, December 2019, 100260, p. 25
- [3] Fischer S. Geogrid reinforcement of ballasted railway superstructure for stabilization of the railway track geometry – A case study. *Geotextiles and Geomembranes*, Volume 50, Issue 5, 2022, pp. 1036-1051
- [4] Sañudo R, Dell'Olio L, Casado J. A, Carrascal I. A, Diego S. Track transitions in railways: A review. *Construction and Building Materials* 112. 2016, pp. 140-157
- [5] Li D, Davis D. Transition of railroad bridge approaches. *Journal of Geotechnical and Geoenvironmental Engineering*. 2005, 131, pp. 1392-1398
- [6] Banimahd M, Woodward P. K, Kennedy J, Medero G. M. Behavior of train-track interaction in stiffness transitions. In *Proceedings of the Institution of Civil Engineers-Transport*; Thomas Telford Ltd.: London, UK, 2012, Volume 165, pp. 205-214

- [7] Briaud J. L., Tafti S. R. High Speed Trains Geotechnics: What is a Tolerable Bump?, *Procedia Engineering*, Volume 189, 2017, pp. 186-192
- [8] Li W, Hou W, Mishra D, Tutumluer E. Modeling the Dynamic Behavior of Track Transitions Along Shared Track Corridors. *Frontiers in Built Environment*, 7:693744, 2021, p. 16
- [9] Zhang X, Zhao C, Zhai W, Shi C, Feng Y. Investigation of track settlement and ballast degradation in the high-speed railway using a full-scale laboratory test. *Proceedings of the Institution of Mechanical Engineers, Part F: Journal of Rail and Rapid Transit*. 2019, 233(8), pp. 869-881
- [10] European Rail Research Institute. Utrecht. ERRI D 230.1/RP 3. "Bridge ends" "Embankment Structure Transition" State of the Art Report, Nov. 1999
- [11] Kerr A. D, Moroney B. E. Track transition problems and remedies. Paper presented at the the American Railway Engineering Association, Washington, USA, 1993
- [12] Sasaoka C. D, Davis D. Implementing track transition solutions for heavy axle load service. Paper presented at the AREMA 2005 Annual Conference, AREMA, 2005
- [13] Li D, Otter D, Carr G. Railway bridge approaches under heavy axle load traffic: problems, causes, and remedies. Paper presented at the Institution of Mechanical Engineers, Part F: *Journal of Rail and Rapid Transit*, 2010, <https://doi.org/10.1243/09544097JRRT345>
- [14] Correia A. G, Cunha J, Marcelino J. L. Caldeira J. Varandas Z. Dimitrovová A. A, Silva M. G. d, Dynamic analysis of rail track for high speed trains. 2D approach. 5th Intl Worksop on Application of Computational Mechanics on Geotechnical Engineering, Portugal, 2007, p. 14
- [15] Banimahd M, Woodward P. K, Kennedy J, Medero G. Behaviour of train-track interaction in stiffness transitions. *Proc. Inst. Civil Eng. Transport* 165, pp. 205-214, doi:10.1680/tran.10.00030); 2012
- [16] Costa D. A, Sofia E. A, Potvin R, Laurans E, Funfschilling C. Railway transitional zones: a case history from ballasted to ballastless track. *Int. J. Railway Tech.* 3 (1), 2014. pp. 37-61, doi:10.4203/ijrt.3.1.2)
- [17] Paixão A, Varandas J. N, Fortunato E, Calçada R. Numerical simulations to improve the use of under sleeper pads at transition zones to railway bridges. *Eng. Structures* 164, 2018, pp. 169-182, doi: 10.1016/j.engstruct.2018.03.005
- [18] Paixão A, Fortunato E, Calçada R. A numerical study on the influence of backfill settlements in the train/track interaction at transition zones to

- railway bridges. Proc. Inst. Mech. Eng. Part F J. Rail. Rapid Transit. 230 (3), 2016, pp. 866-878, doi:10.1177/0954409715573289
- [19] Stark T. D, Wilk S. T. Root cause of differential movement at bridge transition zones. Proc. Inst. Mech. Eng. Part F J. Rail. Rapid Transit. 230 (4), 2016, pp. 1257-1269, doi:10.1177/0954409715589620
- [20] Szepesházi R. Development of bridge substructure design, 50. Bridge Engineering Conference, Siófok, 2009. pp. 429-470
- [21] Laufer I. Soil-structure interaction at bridge abutment, 5th Kézdi Árpád Conference, Budapest, 2017, pp. 143-163
- [22] Koch E, Hudacsek P, Wolf Á. Validated 3D FEM analysis of the geotechnical performance of a semi-integral bridge In: Rahman, Mizanur; Jaksa, Mark Proceedings of the 20th International Conference on Soil Mechanics and Geotechnical Engineering. Sydney, Ausztrália: Australian Geomechanics Society (2022) 5, 302 p. pp. 763-768
- [23] Brinkgreve R. B. J, Vermeer P. A. PLAXIS-Finite element code for soil and rock analyses, Plaxis 3D Manuals, 2010, Delft University of Technology & Plaxis bv, The Netherlands
- [24] Ahmed A, Naggari H. N. Soil-structure interaction of integral abutments. Transportation Geotechnics 38, 2023: 100900. p. 15
- [25] Kong B, Cai CS, Zhang Y. Parametric study of an Integral abutment bridge supported by prestressed precast concrete piles. Eng Struct 2016;120:37-48
- [26] Civjan SA, Bonczar C, Brežna SF, DeJong J, Crovo D. Integral Abutment Bridge Behavior: Parametric Analysis of a Massachusetts Bridge. J Bridge Eng 2007;12(1) 64-71
- [27] Schanz T, Vermeer P. A, Bonnier P. G. The hardening soil model: formulation and verification. Beyond 2000 in computational geotechnics, 1999, pp. 281-296
- [28] Brinkgreve R, Engin E, Engin H. K. Validation of empirical formulas to derive model parameters for sands. 2010, 10.1201/b10551-25
- [29] Koch E. Modeling of embankment foundation, PhD dissertation, Széchenyi István University, Győr, 2013
- [30] Fischer S. Investigation of the horizontal track geometry regarding geogrid reinforcement under ballast. Acta Polytechnica Hungarica, 19(3), 2022, pp. 89-101, doi: <https://doi.org/10.12700/APH.19.3.2022.3.8>
- [31] Shahraki M, Sadaghiani M. R. S, Witt K. J, Meier T. 3D modelling of train induced moving loads on an embankment. Plaxis Bulletin, 36, 2014, pp. 10-15
- [32] Koch E, Szepesházi R, Bene K. Laboratory tests and numerical modeling for embankment foundation on weak soils using deep-mixing. In: Monika,

Sulovska (ed.) 11th Slovak Conference on Geotechnical Engineering: Effect of water on geotechnical structures, Bratislava, Szlovákia: Slovenská technická univerzita v Bratislave, 2013, pp. 257-267

- [33] EN 1991-2: Eurocode 1: Actions on structures - Part 2: Traffic loads on bridges. Authority: The European Union Per Regulation 305/2011, Directive 98/34/EC, Directive 2004/18/EC. 2003
- [34] H.1. Railway bridge regulation, H.1.2. Directive, General design specification of railway bridge and other structures, MAÚT, Budapest, 2019